

## THE SPECTRUM OF FREE VIBRATIONS OF A THIN ELASTIC SPHERICAL SHELL

FRITHIOF I. NIORDSON

Department of Solid Mechanics, The Technical University of Denmark,  
Lyngby, Denmark

(Received 11 September 1987; in revised form 2 February 1988)

**Abstract**—This paper considers the spectrum of an open, thin, elastic, spherical shell, i.e. the set of natural frequencies and their distribution. The results are obtained by extending the analysis given by the author in an earlier paper to the high frequency range and provide a background for testing the applicability of approximate methods suggested by earlier investigators. It was discovered, that the spectrum in some cases displayed a band structure. An explanation of this behaviour is given.

### 1. INTRODUCTION

Forced vibration of structures under random loads with a wide spectrum such as, for instance, acoustic loading from a jet, gives rise to the problem of finding the number of natural frequencies of a structure, which lie within a given interval. This problem has been studied for membranes and plates by Courant and Hilbert (1931) and for thin, elastic shells by Bolotin (1963, 1964), Gol'denveizer (1965, 1970), and Gol'denveizer and Lidskii (1974). A survey over earlier work on the structure of the free vibration spectrum of shells of revolution is given by Gol'denveizer (1980). In that paper Gol'denveizer discusses the distribution of frequencies, the qualitative properties of mode shapes at different points of the spectrum, and approximate methods of analysis for various types of vibrations. In particular the applicability of the membrane theory to the problem of free vibrations is examined.

It seems worthwhile to test the assertions made on the basis of approximate methods on a non-trivial case for which the solution of the complete shell equations can be found. In this paper the distribution of natural frequencies of a thin spherical shell with a circular hole is considered.

The basis for this presentation is a previous paper (Niordson, 1984), in which however, the complete analysis was restricted to frequencies for which the determinant equation had two real and two complex roots. For higher frequencies all four roots are real, and in Section 2 the analysis is extended to this case, the high frequency range.

It is known, that there exist extensional modes in open and closed spherical shells, i.e. solutions to the complete set of shell equations, characterized by zero normal deflection and hence no bending. But for an open shell these are sparse and rank high. Thus, for instance, the lowest purely extensional mode for a free hemispherical shell of thickness ratio  $R/h = 100$  is the first torsional mode, which ranks number 158 on the frequency scale.

It is also known, that no true inextensional modes exist. Thus, practically all modes are mixed in the sense, that some energy is stored in bending of the middle surface and some in stretching of it.

In Section 3 the extensional and the bending energies are determined separately for an arbitrary mode. The energy densities are found analytically, and the total energy is computed by numerical integration.

Although there are no pure bending modes, the term *bending modes* will be arbitrarily used for all modes having most of their strain energy in bending. Similarly, the modes for which the stretching of the middle surface accounts for all, or nearly all strain energy, will be called *extensional modes*. The remaining are the *mixed modes*.

Due to the complexity of the complete shell problem, the applicability of approximate methods is of great interest. Natural frequencies derived by the membrane theory can be regarded as a first approximation of a formal asymptotic process, and it is perhaps not

unnatural to expect the set of membrane frequencies to give at least a rough picture of the true spectrum. As already indicated above, one purpose of this paper is to see, if that holds.

In Section 4 the *membrane modes* and their corresponding natural frequencies are determined from a set of reduced shell equations, in which the bending moments and the transverse shear forces are neglected. These are the membrane modes of Lamb (1883).

Numerical results comprising spectra for different shells are given in Section 5.

Sometimes, for open spherical shells, most natural frequencies are found to be concentrated in narrow bands. This rather surprising observation has not been reported earlier, at least not to the knowledge of the author. This band structure of the spectrum is analysed and discussed.

For very high frequencies, the wavelength of the mode becomes very short, and the equations of shell theory, do not apply. Throughout this paper, only that part of the spectrum will be considered, to which shell theory applies.

## 2. VIBRATION ANALYSIS IN THE HIGH FREQUENCY RANGE

The theory for vibrating spherical shells has been given in a previous paper (Niordson, 1984). However, the elements of the frequency determinant were derived for the low frequency range only, i.e. for eigenvalues satisfying the inequality  $\lambda < \lambda_c$ , where the critical value  $\lambda_c$  is of order unity (Section 5).

Here

$$\lambda = \omega^2(1 - \nu^2) \frac{\gamma}{E} R^2 \quad (1)$$

where  $\omega$  is the angular frequency,  $E$  Young's modulus,  $\nu$  Poisson's ratio,  $R$  the radius of the middle surface, and  $\gamma$  the mass density.

The purpose of this section is to determine the elements of the frequency determinant for the high frequency range, i.e. for the case  $\lambda > \lambda_c$ .

One can recall that for  $\lambda > \lambda_c$  all three roots of the reduced frequency equation

$$\Delta^3 + c_2\Delta^2 + c_1\Delta + c_0 = 0 \quad (2)$$

are real. Here

$$\begin{aligned} c_2 &= 4 + \lambda \\ c_1 &= (1 - \nu^2 - \lambda)/k + 5 - \nu^2 + (3 + \nu)\lambda \\ c_0 &= [2(1 - \nu^2) + (1 + 3\nu)\lambda - \lambda^2]/k + 2(1 - \nu^2) + 2(1 + \nu)\lambda \end{aligned} \quad (3)$$

and

$$k = \frac{h^2}{12R^2} \quad (4)$$

where  $h$  denotes the thickness of the shell.

Equation (2) can be written as

$$\prod_{i=1}^3 \left( \Delta - \frac{\beta_i}{R^2} \right) = 0 \quad (5)$$

where in the case  $\lambda > \lambda_c$  all three roots  $\beta_i$  are real.

The solution for the  $m$ th mode can be derived from the scalar potential functions (p. 325 of Niordson (1985))

$$\Xi_m(\theta, \phi) = \Xi(\theta) \cos m\phi \quad (6)$$

and

$$\chi_m(\theta, \phi) = \chi(\theta) \sin m\phi \quad (7)$$

where  $\theta$  is the co-latitude and  $\phi$  the longitude. The  $\phi$ -independent parts of the potential functions are given by

$$\Xi(\theta) = \sum_{i=1}^3 [A_i P_{\sigma_i}^{-m}(\cos \theta) + B_i P_{\sigma_i}^{-m}(\cos(\pi - \theta))] \quad (8)$$

and

$$\chi(\theta) = A_4 P_{\sigma_4}^{-m}(\cos \theta) + B_4 P_{\sigma_4}^{-m}(\cos(\pi - \theta)). \quad (9)$$

The functions  $P_{\sigma_i}^{-m}$  are the associated Legendre functions of the first kind, of degree  $\sigma_i$ , and order  $-m$ .

The degree  $\sigma_i$  is the solution of

$$-\sigma_i(\sigma_i + 1) = \beta_i, \quad i = 1, 2, 3 \quad (10)$$

and

$$-\sigma_4(\sigma_4 + 1) = 2 \left( 1 + \frac{\lambda}{1 - \nu} \right). \quad (11)$$

From  $\Xi$  one can derive the potential  $\Psi$ , given by (p. 324 of Niordson (1985))

$$\Psi = \frac{1 + \nu}{R} \Xi. \quad (12)$$

All relevant quantities, kinematic as well as static, are found successively from the potential functions (pp. 312–316 of Niordson (1985)). Thus the displacements tangent to the middle surface in the directions of the longitudes and latitudes are

$$u = \frac{1}{R} \left[ \Psi' - \frac{m}{\sin \theta} \chi \right] \cos m\phi \quad (13)$$

and

$$v = \frac{1}{R} \left[ \chi' - \frac{m}{\sin \theta} \Psi \right] \sin m\phi \quad (14)$$

respectively. Here ( )' denotes the partial derivative with respect to  $\theta$ . The displacement normal to the middle surface is (p. 324 of Niordson (1985))

$$w = -\frac{1}{R^2} \left[ \Xi'' + \cot \theta \Xi' + \left( 1 - \nu + \lambda - \frac{m^2}{\sin^2 \theta} \right) \Xi \right] \cos m\phi \quad (15)$$

and the rotation of the normal is given by

$$\psi = \frac{\partial w}{\partial n} = -\frac{1}{R^2} \left[ \Xi''' + \cot \theta \Xi'' + \left( 1 - \nu + \lambda - \frac{1 + m^2}{\sin^2 \theta} \right) \Xi' + \frac{2m^2 \cot \theta}{\sin^2 \theta} \Xi \right] \cos m\phi. \quad (16)$$

The membrane tensile stress  $N$  and shear stress  $S$  are respectively given by (pp. 315–316 of Niordson (1985))

$$N = \frac{Eh}{(1-\nu^2)R^2} \left[ \Psi'' + \nu \cot \theta \Psi' - \frac{\nu m^2}{\sin^2 \theta} \Psi + \frac{m(1-\nu)}{\sin \theta} (\chi \cot \theta - \chi') + R(1+\nu)\bar{w} \right] \cos m\phi \tag{17}$$

and

$$S = \frac{Eh}{2(1+\nu)R^2} \left[ \chi'' - \cot \theta \chi' + \frac{m^2}{\sin^2 \theta} \chi + \frac{2m}{\sin \theta} (\Psi \cot \theta - \Psi') \right] \sin m\phi. \tag{18}$$

Finally, the transverse shear force  $Q$  and the bending moment  $M$  can be determined from (p. 298 of Niordson (1985))

$$Q = -\frac{D}{R^3} \left[ \bar{w}''' + \cot \theta \bar{w}'' + \left( 1 - \cot^2 \theta - \frac{m^2(2-\nu)}{\sin^2 \theta} \right) \bar{w}' + \frac{m^2(3-\nu) \cot \theta}{\sin^2 \theta} \bar{w} \right] \cos m\phi \tag{19}$$

and

$$M = \frac{D}{R^2} \left[ \bar{w}'' + \nu \cot \theta \bar{w}' + \left( 1 + \nu - \frac{\nu m^2}{\sin^2 \theta} \right) \bar{w} \right] \cos m\phi. \tag{20}$$

The notation  $\bar{w}$  has been used here to denote the  $\phi$ -independent factor of  $w$ , i.e.

$$w(\theta, \phi) = \bar{w}(\theta) \cos m\phi.$$

Substitution of eqns (8) and (9) into eqns (12)–(20) yields

$$X = C_X \sum_{i=1}^4 (A_i c_{Xi} + B_i d_{Xi}) \tag{21}$$

where  $X$  stands for any of the quantities

$$u, v, w, \psi, N, S, Q, M.$$

The coefficient  $C_X$  and all 64 functions  $c_{Xi}$  and  $d_{Xi}$  are listed in Appendix A. The tools for computing the eigenvalues  $\lambda$  for  $\lambda > \lambda_c$  are thereby prepared.

Considerations will now be restricted to spherical bowls, i.e. shells containing the pole  $\theta = 0$  and having a boundary at  $\theta = \alpha < \pi$ . Due to the singular behaviour of the associated Legendre functions  $P_{\sigma}^{-m}(x)$  at  $x = -1$ , the coefficients  $B_1, B_2, B_3$ , and  $B_4$  must be zero.

Boundary conditions may be given in statical, kinematical or mixed form. For a spherical bowl with a free boundary, for example, the frequency determinant is

$$D(\lambda) \equiv \begin{vmatrix} c_{N1} & c_{N2} & c_{N3} & c_{N4} \\ c_{S1} & c_{S2} & c_{S3} & c_{S4} \\ c_{M1} & c_{M2} & c_{M3} & c_{M4} \\ c_{Q1} & c_{Q2} & c_{Q3} & c_{Q4} \end{vmatrix} \tag{22}$$

where the elements are given in Niordson (1984) for  $\lambda < \lambda_c$  and in Appendix A for  $\lambda > \lambda_c$ . In all cases they are evaluated at  $\theta = \alpha$ .

The roots of

$$D(\lambda) = 0 \quad (23)$$

are the eigenvalues for that shell. For each integer  $m$  there is an infinite number of roots of eqn (23), and the totality of eigenvalues for all  $m$  constitutes the spectrum of free vibrations.

### 3. THE STRAIN ENERGY OF THE SHELL

In the classical Love–Kirchhoff shell theory, the total strain energy of the deformed shell consists of two parts. The first one,  $W_S$ , is due to the stretching of the middle surface, and the second part,  $W_B$ , is due to bending. One has

$$W_S = \frac{EhR^2}{2(1-\nu^2)} \int_0^{2\pi} \int_{\alpha_1}^{\alpha_2} [(\varepsilon_{11} + \varepsilon_{22})^2 - 2(1-\nu)(\varepsilon_{11}\varepsilon_{22} - \varepsilon_{12}^2)] \sin \theta \, d\theta \, d\phi \quad (24)$$

and

$$W_B = \frac{DR^2}{2} \int_0^{2\pi} \int_{\alpha_1}^{\alpha_2} [(\kappa_{11} + \kappa_{22})^2 - 2(1-\nu)(\kappa_{11}\kappa_{22} - \kappa_{12}^2)] \sin \theta \, d\theta \, d\phi \quad (25)$$

where  $\varepsilon_{11}$ ,  $\varepsilon_{12}$ , and  $\varepsilon_{22}$  are the physical strain components of the middle surface and  $\kappa_{11}$ ,  $\kappa_{12}$ , and  $\kappa_{22}$  the physical components of bending. The boundaries of the spherical zone are given by the co-latitudes  $\alpha_1$  and  $\alpha_2$ .

When eqns (6) and (7) are substituted into the relevant formulae for extension and bending (eqns (3.11) and (3.37) of Niordson (1985)) one obtains

$$\varepsilon_{11} = \frac{1}{R^2} \left[ \Psi'' - \frac{m}{\sin \theta} (\chi' - \cot \theta \chi) + R\bar{w} \right] \cos m\phi \quad (26)$$

$$\varepsilon_{12} = \frac{1}{2R^2} \left[ \chi'' - \cot \theta \chi' + \frac{m^2}{\sin^2 \theta} \chi - \frac{2m}{\sin \theta} (\Psi' - \cot \theta \Psi) \right] \sin m\phi \quad (27)$$

$$\varepsilon_{22} = \frac{1}{R^2} \left[ \frac{m}{\sin \theta} (\chi' - \cot \theta \chi) + \cot \theta \Psi' - \frac{m^2}{\sin^2 \theta} \Psi + R\bar{w} \right] \cos m\phi \quad (28)$$

and

$$\kappa_{11} = \frac{1}{R^2} (\bar{w}'' + \bar{w}) \cos m\phi \quad (29)$$

$$\kappa_{12} = \frac{m}{R^2 \sin \theta} (\cot \theta \bar{w}' - \bar{w}') \sin m\phi \quad (30)$$

$$\kappa_{22} = \frac{1}{R^2} \left[ \cot \theta \bar{w}' + \left( 1 - \frac{m^2}{\sin^2 \theta} \right) \bar{w} \right] \cos m\phi. \quad (31)$$

For axisymmetrical modes  $m = 0$  the integration with respect to  $\phi$  gives a factor  $2\pi$  and for  $m > 0$  the corresponding factor is  $\pi$ . The integration in the direction of  $\theta$  cannot be given in closed form, and in the subsequent analysis it is performed numerically.

### 4. MEMBRANE MODES

The membrane solution of the shell equations is the limiting case, when  $k$  approaches zero. Multiplying eqn (1) through by  $k$  and taking the limit, one finds

$$(1 - \nu^2 - \lambda)\Delta + 2(1 - \nu^2) + (1 + 3\nu)\lambda - \lambda^2 = 0. \quad (32)$$

There are two roots less than in the general case of the complete shell equations. The solution is now given by

$$\Xi(\theta) = A_1 P_{\sigma_1}^{-m}(\cos \theta) + B_1 P_{\sigma_1}^{-m}(\cos(\pi - \theta)) \quad (33)$$

and

$$\chi(\theta) = A_4 P_{\sigma_4}^{-m}(\cos \theta) + B_4 P_{\sigma_4}^{-m}(\cos(\pi - \theta)) \quad (34)$$

where

$$\sigma_1(\sigma_1 + 1) = \frac{2(1 - \nu^2) + (1 + 3\nu)\lambda - \lambda^2}{1 - \nu^2 - \lambda} \quad (35)$$

and

$$\sigma_4(\sigma_4 + 1) = -2 \left( 1 + \frac{1}{1 + \nu} \right) \quad (36)$$

as before.

The frequency determinant for a spherical bowl with a free boundary reduces to

$$D(\lambda) \equiv \begin{vmatrix} c_{N1} & c_{N4} \\ c_{S1} & c_{S4} \end{vmatrix} \quad (37)$$

where the elements are given in Niordson (1984) for  $\lambda < \lambda_c$  and in Appendix A for  $\lambda > \lambda_c$ .

Equation (35) shows that  $\lambda = 1 - \nu^2$  is a singular point. In fact, the frequency determinant has an essential singularity at this point. As  $\lambda$  approaches  $1 - \nu^2$  from below, the determinant has zeros within any arbitrary distance from the singularity. For  $\lambda > 1 - \nu^2$ , however, the determinant behaves in a regular way; there is no finite limit point for the zeros in this interval.

For that reason the spectrum of membrane modes will have a finite limit point at  $\lambda = 1 - \nu^2$ . The real spectrum, for sure, does not have such a limit point, nor does the spectrum based upon the shell equations, when the bending moment and the shear force are taken into account.

## 5. NUMERICAL RESULTS

The critical value  $\lambda_c$  divides the spectrum into the low and the high frequency range. It may be defined as that value of  $\lambda$  for which the algebraic equation, eqn (2), has a double root. From this it follows, that it can be determined as the real root of

$$p^3 + q^2 = 0 \quad (38)$$

where

$$p = \frac{1}{3}c_1 - \frac{1}{3}c_2^2 \quad (39)$$

and

Table 1.  $\lambda_c$  as a function of  $R/h$  and  $\nu$ 

$R/h$	$\nu$					
	0	0.1	0.2	0.3	0.4	0.5
25	1.158	1.165	1.150	1.113	1.052	0.966
50	1.098	1.099	1.077	1.034	0.969	0.880
100	1.062	1.058	1.033	0.987	0.919	0.830
200	1.039	1.032	1.006	0.958	0.889	0.800
400	1.024	1.017	0.989	0.940	0.871	0.781

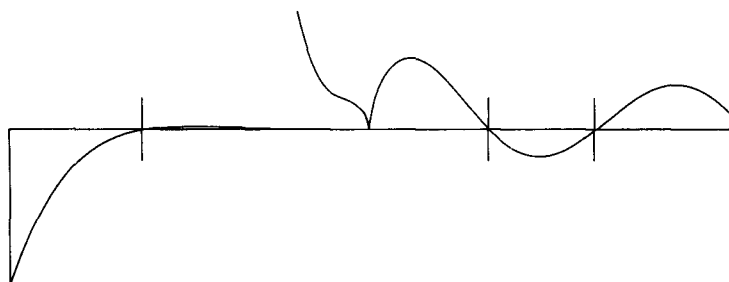


Fig. 1. Frequency determinant as a function of frequency.

$$q = \frac{1}{27}c_2^3 - \frac{1}{6}c_1c_2 + \frac{1}{2}c_0 \quad (40)$$

and is clearly a function of the thickness ratio  $R/h$  and of Poisson's ratio. In Table 1  $\lambda_c$  is given for different values of  $R/h$  and  $\nu$ . Considerations will be restricted to spherical bowls with a free boundary, for which the frequency determinant is given by eqn (22).

The function  $D(\lambda)$  is zero whenever  $\lambda$  is an eigenvalue. In addition  $D(\lambda_c) = 0$ , because at this value eqn (1) has a double root, and hence the four functions

$$P_{\sigma_i}^{-m} \quad (i = 1, \dots, 4)$$

are linearly dependent at the point  $\lambda = \lambda_c$ .

The determinant is an oscillating function with a singularity at  $\lambda = \lambda_c$ . Its behaviour (for a given value of  $m > 1$ ) is illustrated in Fig. 1, which shows  $D$  as a function of  $\lambda$ . The zeros, that are eigenvalues, are indicated by vertical lines.

To make visible the initial as well as the behaviour for larger values of  $\lambda$ , two different scales for  $D$  were used in Fig. 1, one to the left of the apparent discontinuity (which is *no* discontinuity in  $D$ ) and one to the right, where  $D$  has been magnified 300 times.

The zeros, i.e. the eigenvalues, were determined in the following way. The wave number  $m$  was held constant, and  $\lambda$  was increased in appropriately small steps, until a change of sign of the determinant did signal the presence of an eigenvalue in the last interval. By decreasing  $\lambda$  using smaller steps, and repeating the process whenever the determinant changed sign, the eigenvalue was trapped with the accuracy desired.† The associated Legendre functions are evaluated by the method described in Niordson (1984).

Of course, care has to be taken to make the first step small enough, so that it does not contain more than one zero. This can only be done by a careful numerical study of the behaviour of the determinant.

The number of zeros‡ was given the modal number  $j$ .

At the point  $\lambda = \lambda_c$  in Fig. 1, the curve reaches the abscissa with a vertical tangent. By properly selecting the sign of the analytical expression (22) for  $\lambda > \lambda_c$ ,  $D$  does not change sign there. Therefore, this point cannot be mistaken for an eigenvalue.

The natural frequencies depend on the thickness of the shell and on the size of the

† The requirement was one part in  $10^9$  in all cases reported below.

‡ For  $m = 0$  and 1 the frequency equation has a double and a single root, respectively, at frequency zero, corresponding to the modes of rigid body motion. These zeros are also counted.

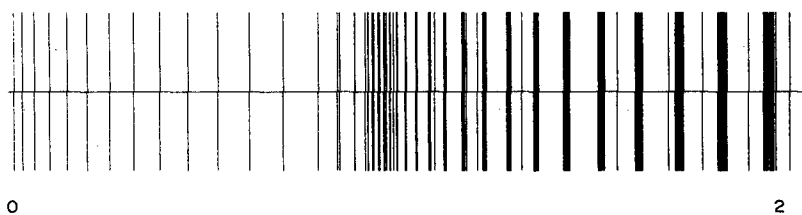


Fig. 2(a). Complete spectrum of a hemispherical shell.

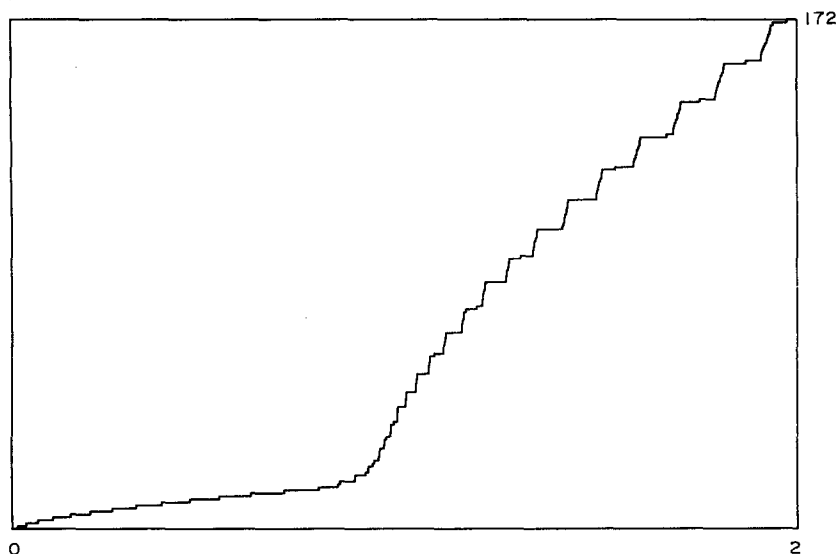


Fig. 2(b). Number of natural frequencies below a given frequency.

opening, determined by the co-latitude  $\alpha$ . The dependence on Poisson's ratio  $\nu$  is small and not investigated here. Therefore, in all subsequent calculations, Poisson's ratio was assigned the arbitrarily selected value 0.3.

### 5.1. Hemispherical shell

In this subsection numerical results of a hemispherical shell of thickness ratio  $R/h = 100$  are discussed.

The Love-Kirchhoff first-order shell theory has inherent errors of order  $O(h/R) + O(h^2/L^2)$ , where  $L$  is a characteristic wavelength of the deformation pattern. The first term is due to neglecting the coupling of the extensional and bending energies, and the second one is due to neglecting the shear of the normals. As long as  $L$  is not less than  $10h$  the second term will not predominate. It seems therefore reasonable to restrict the analysis for this shell to such modes, for which  $L$  is greater than  $10h$ . Since the circumference is  $200\pi h$ , to fulfil this requirement, the mode number  $m$  should be less than  $10\pi$ , which means, that there must be less than  $20\pi$  nodes in the circumferential direction. For the same reason,  $j$  should not exceed 15.

To go above this range, one must take  $m > 25$  or  $j > 16$ . This range may therefore be claimed to cover the whole range to which shell theory can be applied.

In Appendix B the 172 lowest natural frequencies are given together with their corresponding modal numbers and the percentage of extensional energy associated with the mode. These fulfil the requirements  $m < 25$  and  $j < 15$ , and are in fact all eigenvalues below the value of 4.

In Table 1 the frequencies are given in dimensionless form as the square root of the eigenvalue, i.e.



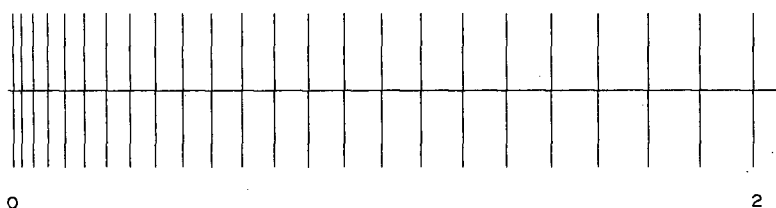


Fig. 3(a). Spectrum of bending modes.

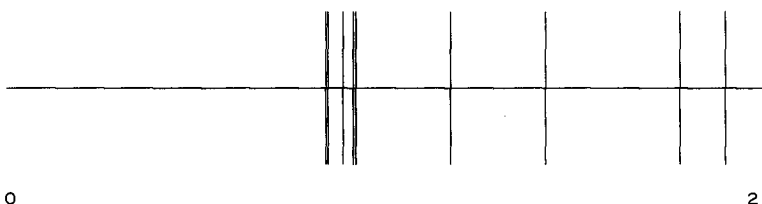


Fig. 3(b). Spectrum of extensional modes.

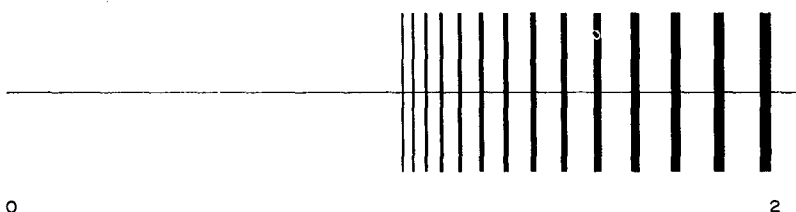


Fig. 3(c). Spectrum of the remaining (mixed) modes.

$$\Omega = \sqrt{\lambda} = \omega R \sqrt{\left( (1-\nu^2) \frac{\gamma}{E} \right)}.$$

In Fig. 2(a) the frequencies are shown in the conventional form of a spectrum and in Fig. 2(b) as the number of frequencies  $N(\Omega)$  below a given frequency  $\Omega$ .

In the low frequency range the natural frequencies show a regular pattern with regularly increasing intervals. From right below the critical value, the spectrum becomes more dense and irregular. However, in the high frequency range, there is a remarkable band structure. In this region, most of the frequencies belong to comparatively narrow, densely filled bands, interspersed with regions that are empty or almost empty.

The *bending modes* are characterized by the modal numbers  $j = 1$  and  $m > 1$ . There are 24 bending modes in the frequency range considered. In the lowest mode the energy due to stretching of the middle surface amounts to only 1.7% of the total strain energy. With increasing mode number, this ratio increases, reaches a maximum of 21.8% at mode number 12, and decreases thereafter monotonously towards zero. In the last mode considered, it has fallen to 8.5%.

This can be understood, if one considers that in a shell with double curvature, bending must be accompanied by stretching of the middle surface. The more bending, the more stretching, and hence the energy due to stretching will tend to increase with the mode number. However, with increasing  $m$  the penetration of the bending from the free boundary decreases, and for very high values of  $m$  only a narrow boundary zone suffers deformation. Such a narrow zone of a hemispherical shell is almost cylindrical, i.e. the curvature in the lateral direction is hardly felt, and inextensional deformation can therefore be closely approximated.

The spectrum of the bending modes is shown in Fig. 3(a). It looks much like the corresponding spectra of beams and plates, i.e. with regularly increasing intervals.

If the *extensional modes* are defined as modes having *no* energy in bending at all, there is only one such mode in the frequency range considered (No. 158, with the modal numbers  $m = 0$  and  $j = 14$ ). This mode corresponds to axisymmetrical shear with one nodal circle.

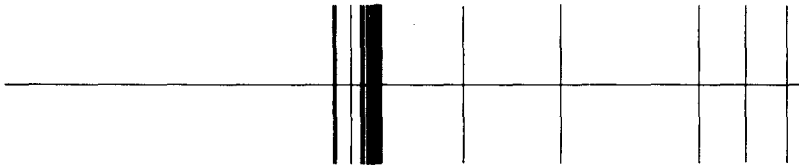


Fig. 4. Spectrum of membrane modes.

The remaining three modes in the table showing 100.0% extensional energy are not completely free from bending. The figures are rounded off, the ratios being above 99.95 but actually below 100%.

However, if modes with a percentage of say, more than 98.9 are regarded as extensional, 25 such modes can be recorded. Their spectrum is shown in Fig. 3(b). Only 5 of them belong to the high frequency range, the rest are found in the upper end of the low frequency range.

All remaining modes will be referred to as *mixed modes*. They constitute a majority of 126, and their spectrum is shown in Fig. 3(c). A most remarkable fact is the very regular appearance of this spectrum. The bands are dense and interspersed with regularly increasing intervals. Another regularity is perhaps less evident. For most of the modes belonging to a band the characteristic number of it,  $m + 2j$  is the same.

The reasons for the band structure and its regular appearance will be discussed further below.

For the same shell, the spectrum of the *membrane modes*, computed according to the theory in Section 4 is given in Fig. 4. If one disregards the misleading density of frequencies in the vicinity of the finite limit point in this spectrum of membrane modes, it gives a fair picture of the true spectrum of extensional modes. However, the vast majority of natural frequencies, consisting of all mixed and all bending modes, is completely missing. The membrane modes represent just a tiny fraction of the complete set.

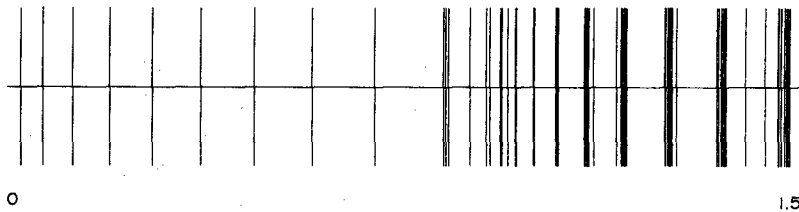


Fig. 5(a). Complete spectrum for 90°.

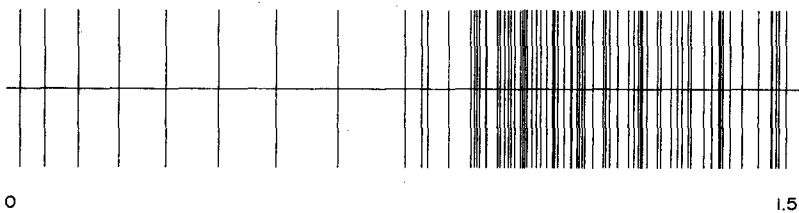


Fig. 5(b). Complete spectrum for 110°.

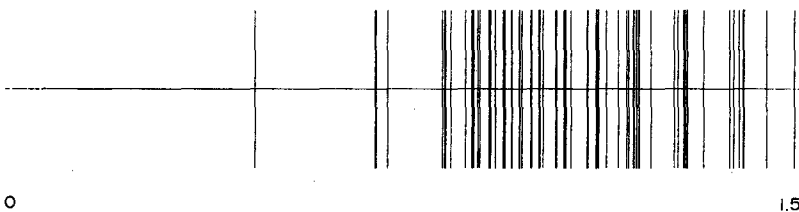
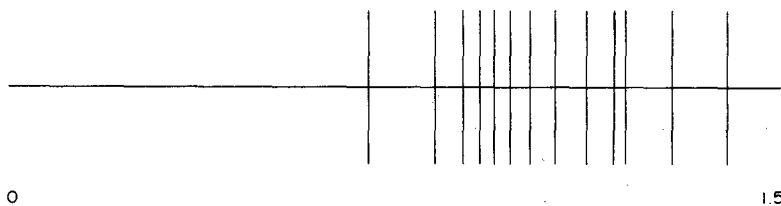
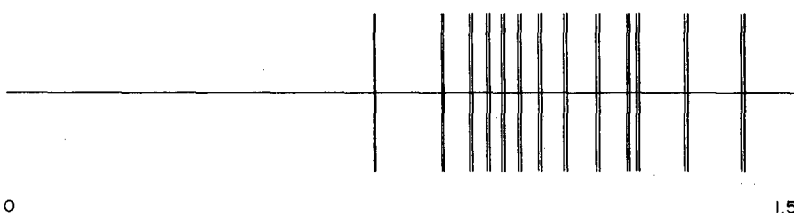


Fig. 5(c). Complete spectrum for 170°.

Table 2. Frequencies of a spherical shell of thickness ratio  $R/h = 50$ 

No.	$\Omega$	$n$	Class
1	0.7012	2	II
2	0.8318	3	II
3	0.8863	4	II
4	0.9193	5	II
5	0.9473	6	II
6	0.9782	7	II
7	1.0165	8	II
8	1.0654	9	II
9	1.1272	10	II
10	1.1832	3	I
11	1.2035	11	II
12	1.2954	12	II
13	1.4032	13	II

Fig. 6(a). Complete spectrum for  $180^\circ$ .Fig. 6(b). Complete spectrum for  $177^\circ$ .

### 5.2. The band structure

In this subsection the structure of the spectrum of a spherical bowl is analysed, especially the appearance of bands. For that purpose a shell of thickness ratio  $R/h = 50$  is taken, and the influence of the size of the opening, i.e. the influence of  $\alpha$  is considered.

For a hemispherical shell  $\alpha = 90^\circ$  the first 65 natural frequencies, covering the range  $0 < \Omega < 1.5$  are shown in Fig. 5(a). The band structure of the high frequency range is apparent also in this case. When  $\alpha$  is increased or decreased, the bands broaden and dissolve. Thus, in the spectrum for  $\alpha = 110^\circ$  (Fig. 5(b)) the bands can hardly be distinguished.

With a further increase of  $\alpha$ , new bands begin to form and for  $\alpha = 170^\circ$  (Fig. 5(c)) most of the 106 frequencies in the range considered, have been rearranged into new bands.

The explanation for the band structure is now close at hand. For  $\alpha = 180^\circ$  the shell is closed with no free boundary. The modes are the tesseral ( $m < n$ ) and sectoral ( $m = n$ ) surface harmonics (pp. 317–319 of Niordson (1984))

$$P_n^m \cos(m\phi)$$

where  $n \geq m$ .

For each integer  $n > 0$  there is one axisymmetrical mode and  $n$  non-axisymmetrical modes, given by  $m = 0, 1, 2, \dots, n$  corresponding to the surface harmonics of order  $m$ . The frequency, however, depends only on  $n$ , since due to spherical symmetry any mode having a mode number  $m > 0$  can be obtained by superposing a number of axisymmetrical modes of degree  $n$ , with properly chosen axes and amplitudes.

There are 13 of them in the range considered, one of the *first class* and twelve of the *second class*.† They are given in Table 2 and their spectrum is shown in Fig. 6(a).

† This is the terminology of Lamb (1883). The modes of the first class are purely extensional, and their frequency is independent of the thickness of the shell.

For each  $n$  there are  $n+1$  modes and in this range there are therefore 106 different modes.

A hole, no matter how small, will destroy the spherical symmetry, and the frequencies split into bands, the narrower the smaller the hole.

Thus, for a hole of radius  $3^\circ$ , i.e. for  $\alpha = 177^\circ$ , there are 106 distinct frequencies in the range considered, and, as one would expect, they are found in narrow bands, close to the frequencies of the complete shell (Fig. 6(b)).

Each band appears as a double line in the spectrum. The first line is the single mode  $m = 2$ , and the second line is actually a narrow band containing the remaining  $n$  different frequencies. Within each band, including the single line, the number  $m+j$  is the same.

The band structure of a spherical shell with a small hole has thus a simple explanation.

The modes of a complete spherical shell, if properly oriented, are either symmetrical or antisymmetrical with respect to the equator. For any axisymmetrical mode connected with a symmetrical normal stress field, the interaction between the two hemispheres of a complete shell is through the bending moment or the shear forces at the equator only, and only if they are non-vanishing.

For such modes, the frequencies of a complete spherical shell will be approximately the same as the frequencies of its two hemispherical parts, the difference being due to bending. But since bending is either non-existent or contributes only slightly to the energy of the complete shell, the images of such modes on the hemispherical shell will be found in narrow bands.

Since there are half as many nodal latitudes on the hemisphere as on the complete sphere, the characteristic number for a band, being  $m+j$  for the sphere, is  $m+2j$  for the hemisphere.

## 6. DISCUSSION

The results presented in this paper show that approximate methods based on the membrane theory are inadequate for predicting the distribution of natural frequencies of a spherical shell.

Two reasons can be given. First, the membrane theory predicts a limit point for the frequencies at the upper end of the low frequency range, when in fact no finite limit point exists.

Secondly, for frequencies in the high frequency range, up to the limit set by the approximate nature of shell theory, the membrane solution represents only a small fraction of the frequencies actually present.

## REFERENCES

- Bolotin, V. V. (1963). On the density of the distribution of natural frequencies. *P.M.M.* **27**(2), 538–543.
- Bolotin, V. V. (1964). On the broadband random vibration of elastic systems. *Proc. 11th Int. Cong. Appl. Mech.*, Munich, 1964, pp. 233–238. Springer, Berlin.
- Courant, R. and Hilbert, D. (1931). *Methoden der Mathematischen Physik*, 2nd Edn, Vol. 1, pp. 373–387. Springer, Berlin.
- Gol'denveizer, A. L. (1965). Qualitative analysis of free vibrations of an elastic thin shell. *P.M.M.* **30**(1), 110–127.
- Gol'denveizer, A. L. (1970). On the frequency distribution density of oscillations of a thin shell. *P.M.M.* **34**(5), 910–915.
- Gol'denveizer, A. L. and Lidskii, V. B. (1974). Some general properties of the free vibrations of a thin elastic shell. *Isv. AN SSSR Meckhanika Tverdogo Tela* **9**(2), 108–112.
- Gol'denveizer, A. L. (1980). Free vibration spectrum structure of a shell of revolution. *Mech. Today* **5**, 67–82.
- Lamb, H. (1883). On the vibrations of a spherical shell. *Lond. Math. Soc. Proc.* **14**, 50.
- Niordson, F. I. (1984). Free vibrations of thin elastic spherical shells. *Int. J. Solids Structures* **20**, 667–687.
- Niordson, F. I. (1985). *Shell Theory*, p. 408. North Holland, Amsterdam.

## APPENDIX A

The coefficients of the frequency determinant are obtained in eqn (21). In order to write them in a compact form, the following notation will be used:

$$\begin{aligned} \alpha_1 &= \frac{m(m+1)}{\sin^2 \theta}, & \alpha_4 &= \lambda + 1 - \nu \\ \alpha_2 &= \alpha_1 - m - 1 - \frac{\lambda}{1 - \nu}, & \alpha_5 &= (1 - \nu)\alpha_1 - 2 \\ \alpha_3 &= (1 - \nu)(\alpha_1 - m - 1) + 2, & \alpha_6 &= \frac{(1 - \nu)m^2}{\sin^2 \theta} - 2 \\ D &= \frac{Eh^3}{12(1 - \nu^2)}. \end{aligned}$$

For  $i = 1, 2, 3, 4$ , let

$$\begin{aligned} P_i &= P_{\sigma_i}^{-m}(\cos \theta), & \hat{P}_i &= P_{\sigma_i}^{-m}(\cos(\pi - \theta)) \\ P_i^1 &= P_{\sigma_i}^{-m+1}(\cos \theta), & \hat{P}_i^1 &= P_{\sigma_i}^{-m+1}(\cos(\pi - \theta)). \end{aligned}$$

Then the coefficients can be written as follows, where the range of index  $i$  is 1, 2, 3

$$\begin{aligned} C_N &= \frac{Eh}{R^3} \\ c_{Ni} &= \alpha_2 P_i - \cot \theta P_i^1 \\ c_{N4} &= \frac{1}{1 + \nu} \left[ \alpha_1 \cos \theta P_4 - \frac{m}{\sin \theta} P_4^1 \right] \\ d_{Ni} &= \alpha_2 \hat{P}_i + \cot \theta \hat{P}_i^1 \\ d_{N4} &= \frac{1}{1 + \nu} \left[ \alpha_1 \cos \theta \hat{P}_4 + \frac{m}{\sin \theta} \hat{P}_4^1 \right] \\ C_S &= \frac{Eh}{R^3} \\ c_{Si} &= \alpha_1 \cos \theta P_i - \frac{m}{\sin \theta} P_i^1 \\ c_{S4} &= \frac{1}{1 + \nu} [(\alpha_1 - m - \frac{1}{2}\beta_4) P_4 - \cot \theta P_4^1] \\ d_{Si} &= \alpha_1 \cos \theta \hat{P}_i + \frac{m}{\sin \theta} \hat{P}_i^1 \\ d_{S4} &= \frac{1}{1 + \nu} [(\alpha_1 - m - \frac{1}{2}\beta_4) \hat{P}_4 + \cot \theta \hat{P}_4^1] \\ C_M &= \frac{D}{R^4} \\ c_{Mi} &= -(\alpha_4 - \beta_i)[(\alpha_3 - \beta_i) P_i - (1 - \nu) \cot \theta P_i^1] \\ d_{Mi} &= -(\alpha_4 - \beta_i)[(\alpha_3 - \beta_i) \hat{P}_i + (1 - \nu) \cot \theta \hat{P}_i^1] \\ c_{M4} &= d_{M4} = 0 \\ C_Q &= \frac{D}{R^5} \\ c_{Qi} &= (\alpha_4 - \beta_i)[(\alpha_5 + \beta_i)m \cot \theta P_i^1 - (\alpha_6 + \beta_i) P_i] \\ d_{Qi} &= -(\alpha_4 - \beta_i)[(\alpha_5 + \beta_i)m \cot \theta \hat{P}_i + (\alpha_6 + \beta_i) \hat{P}_i^1] \\ c_{Q4} &= d_{Q4} = 0 \\ C_u &= \frac{1}{R^2} \\ c_{ui} &= (1 + \nu)[P_i^1 - m \cot \theta P_i] \\ c_{u4} &= -\frac{m}{\sin \theta} P_4 \\ d_{ui} &= (1 + \nu)[\hat{P}_i^1 + m \cot \theta \hat{P}_i] \\ d_{u4} &= \frac{m}{\sin \theta} \hat{P}_4 \end{aligned}$$

$$C_v = \frac{1}{R^2}$$

$$c_{vi} = -(1+\nu) \frac{m}{\sin \theta} P_i$$

$$c_{v4} = -m \cot \theta P_4 + P_4^1$$

$$d_{vi} = (1+\nu) \frac{m}{\sin \theta} \hat{P}_i$$

$$d_{v4} = m \cot \theta \hat{P}_4 + \hat{P}_4^1$$

$$C_w = \frac{1}{R^2}$$

$$c_{wi} = (\beta_i - \alpha_4) P_i$$

$$d_{wi} = (\beta_i - \alpha_4) \hat{P}_i$$

$$c_{w4} = d_{w4} = 0$$

$$C_\psi = \frac{1}{R^3}$$

$$c_{\psi i} = (\alpha_4 - \beta_i) [m \cot \theta P_i - P_i^1]$$

$$d_{\psi i} = (\alpha_4 - \beta_i) [-m \cot \theta \hat{P}_i - \hat{P}_i^1]$$

$$c_{\psi 4} = d_{\psi 4} = 0.$$

APPENDIX B

Frequencies of a hemispherical shell of thickness ratio  $R/h = 100$

No.	$\Omega$	$m$	$j$	$W_s$	No.	$\Omega$	$m$	$j$	$W_s$
1	0.0123	2	1	1.7	41	0.9832	6	3	91.4
2	0.0339	3	1	3.2	42	1.0028	9	2	88.1
3	0.0640	4	1	5.0	43	1.0030	1	6	88.4
4	0.1017	5	1	7.2	44	1.0038	3	5	88.2
5	0.1462	6	1	9.7	45	1.0048	5	4	88.0
6	0.1968	7	1	12.5	46	1.0051	7	3	87.8
7	0.2531	8	1	15.2	47	1.0290	0	8	84.3
8	0.3146	9	1	17.6	48	1.0291	10	2	83.9
9	0.3810	10	1	19.6	49	1.0294	2	6	84.2
10	0.4521	11	1	21.0	50	1.0306	4	5	84.0
11	0.5277	12	1	21.7	51	1.0318	6	4	83.7
12	0.6078	13	1	21.8	52	1.0320	8	3	83.6
13	0.6923	14	1	21.4	53	1.0609	1	7	79.5
14	0.7813	15	1	20.6	54	1.0612	11	2	79.0
15	0.8304	0	3	99.9	55	1.0619	3	6	79.4
16	0.8361	1	2	99.9	56	1.0634	5	5	79.1
17	0.8748	16	1	19.5	57	1.0648	9	3	78.7
18	0.8752	2	2	99.7	58	1.0648	7	4	78.8
19	0.9018	3	2	99.4	59	1.0758	18	1	16.9
20	0.9087	0	4	99.3	60	1.0992	0	9	74.3
21	0.9092	1	3	99.4	61	1.0997	2	7	74.2
22	0.9202	4	2	99.8	62	1.0998	12	2	73.5
23	0.9238	2	3	98.8	63	1.1011	4	6	74.0
24	0.9349	5	2	97.8	64	1.1030	6	5	73.7
25	0.9370	3	3	97.8	65	1.1041	10	3	73.2
26	0.9379	0	5	98.5	66	1.1045	8	4	73.4
27	0.9385	1	4	98.0	67	1.1448	1	8	68.6
28	0.9488	6	2	96.3	68	1.1456	13	2	67.6
29	0.9503	4	3	96.3	69	1.1458	3	7	68.5
30	0.9507	2	4	96.5	70	1.1477	5	6	68.2
31	0.9548	0	6	97.3	71	1.1498	7	5	67.9
32	0.9638	7	2	94.3	72	1.1507	11	3	67.3
33	0.9650	1	5	94.5	73	1.1513	9	4	67.6
34	0.9652	3	4	94.4	74	1.1559	2	8	100.0
35	0.9653	5	3	94.2	75	1.1836	19	1	15.5
36	0.9730	17	1	18.2	76	1.1977	0	10	62.8
37	0.9814	8	2	91.5	77	1.1982	2	9	62.7
38	0.9822	2	5	91.8	78	1.1992	14	2	61.4
39	0.9823	0	7	92.0	79	1.1997	4	7	62.6
40	0.9829	4	4	91.5	80	1.2020	6	6	62.3

Frequencies of a hemispherical shell of thickness ratio  $R/h = 100$  (cont.)

No.	$\Omega$	$m$	$j$	$W_s$	No.	$\Omega$	$m$	$j$	$W_s$
81	1.2044	8	5	61.9	127	1.5913	19	2	33.2
82	1.2050	12	3	61.3	128	1.5922	9	7	35.6
83	1.2059	10	4	61.6	129	1.5958	11	6	35.4
84	1.2587	1	9	56.9	130	1.5989	13	5	35.0
85	1.2598	3	8	56.8	131	1.5992	17	3	33.9
86	1.2598	15	2	55.2	132	1.6005	15	4	34.5
87	1.2617	5	7	56.6	133	1.6662	23	1	10.5
88	1.2643	7	6	56.4	134	1.6837	0	13	32.0
89	1.2669	9	5	56.0	135	1.6842	2	12	32.4
90	1.2673	13	3	55.2	136	1.6857	4	10	31.9
91	1.2684	11	4	55.6	137	1.6882	6	9	31.8
92	1.2964	20	1	14.1	138	1.6914	8	8	31.6
93	1.3275	0	11	51.2	139	1.6848	20	2	28.8
94	1.3280	2	10	51.2	140	1.6952	10	7	31.4
95	1.3295	4	8	51.1	141	1.6991	12	6	31.2
96	1.3308	16	2	49.1	142	1.7022	14	5	30.8
97	1.3320	6	7	50.9	143	1.7027	18	3	29.7
98	1.3349	8	6	50.6	144	1.7040	16	4	30.3
99	1.3376	10	5	50.2	145	1.7527	3	11	100.0
100	1.3378	14	3	49.3	146	1.7927	1	12	28.2
101	1.3391	12	4	49.8	147	1.7936	3	12	28.2
102	1.4026	1	10	98.9	148	1.7956	5	10	28.1
103	1.4056	3	9	45.7	149	1.7985	7	9	28.0
104	1.4077	5	8	45.6	150	1.8004	24	1	9.4
105	1.4092	17	2	43.4	151	1.8019	9	8	27.9
106	1.4105	7	7	45.4	152	1.8061	11	7	27.7
107	1.4137	9	6	45.1	153	1.8063	21	2	25.0
108	1.4143	21	1	12.8	154	1.8100	13	6	27.4
109	1.4165	11	5	44.7	155	1.8135	15	5	27.0
110	1.4167	15	3	43.8	156	1.8141	19	3	25.9
111	1.4180	13	4	44.3	157	1.8153	17	4	26.6
112	1.4896	0	12	40.8	158	1.8708	0	14	100.0
113	1.4901	2	11	40.7	159	1.9090	0	15	26.9
114	1.4916	4	9	40.7	160	1.9095	2	13	40.4
115	1.4941	6	8	40.5	161	1.9109	4	11	24.9
116	1.4961	18	2	38.0	162	1.9132	6	10	24.8
117	1.4973	8	7	40.3	163	1.9163	8	9	24.8
118	1.5007	10	6	40.0	164	1.9198	10	8	24.6
119	1.5037	12	5	39.6	165	1.9245	12	7	24.4
120	1.5038	16	3	38.6	166	1.9257	22	2	21.7
121	1.5052	14	4	39.1	167	1.9287	14	6	24.1
122	1.5376	22	1	11.6	168	1.9319	16	5	23.8
123	1.5828	1	11	36.1	169	1.9333	20	3	22.6
124	1.5838	3	10	36.1	170	1.9343	18	4	23.3
125	1.5858	5	9	36.0	171	1.9401	25	1	8.5
126	1.5887	7	8	35.9	172	1.9748	0	16	100.0